

Fluid driven cohesive crack propagation in quasi-brittle materials

F. Barpi¹, S. Valente²

Department of Structural and Geotechnical Engineering, Politecnico di Torino,
Corso Duca degli Abruzzi 24, 10129 Torino, Italy.

¹Tel: +39 11 5644886, Fax: +39 11 5644899, e-mail: *fabrizio.barpi@polito.it*

²Tel: +39 11 5644853, Fax: +39 11 5644899, e-mail: *silvio.valente@polito.it*

Keywords: Cohesive, Concrete, Crack, Dam, Fracture, Hydro-Mechanical coupling, Joint, Rock.

SUMMARY. When fracture occurs in a concrete dam, the crack mouth is typically exposed to water. Very often this phenomenon occurs at the dam-foundation joint and is driven also by the fluid pressure inside the crack. Since the joint is the weakest point in the structure, this evolutionary process determines the load bearing capacity of the dam. In this paper the cracked joint is analysed through the cohesive model proposed by Cervenka, Kishen and Saouma which takes into account the coupled degradation of normal and tangential strength. A judicious choice of the mechanical parameters required by the above mentioned model allows us to determine a stress and displacement field at the crack tip that is admissible according to the ICOLD benchmark from both a static and a kinematic point of view.

1 INTRODUCTION

The mechanical behaviour of joints plays a key role in concrete dam engineering since the joint is the weakest point in the structure and therefore the evolutionary crack process occurring along this line determines the global load bearing capacity. In the scientific literature two problems are discussed:

- the problem of sliding along a pre-existing compressed discontinuity (see, among others, [1]),
- the problem of crack initiation and propagation along an undamaged interface (see [2], [3], [4]).

The latter problem is discussed below in the framework of the cohesive crack models, introduced by Barenblatt and Dugdale for elastoplastic materials, and by Hillerborg et al. for quasi-brittle materials. In this model, the nonlinear fracture process zone (due to degradation mechanisms such as plastic micro-voiding or micro-cracking) in front of the actual crack tip is lumped into a discrete line (two-dimensional) or plane (three-dimensional) and is represented by a traction-separation law across this line or plane. In a cohesive crack the stress field is not singular.

2 JOINT MODELS

A joint is a locus of possible displacement discontinuities. The separation phenomenon is analysed in the plasticity framework since an irreversible process occurs. The displacement discontinuity vector \boldsymbol{w} is assumed to be the sum of a reversible (superscript e) and an irreversible (superscript p) contribution:

$$\dot{\boldsymbol{w}} = \dot{\boldsymbol{w}}^e + \dot{\boldsymbol{w}}^p \quad (1)$$

$$\dot{\boldsymbol{p}} = K_0 \dot{\boldsymbol{w}}^e = K_0 (\dot{\boldsymbol{w}} - \dot{\boldsymbol{w}}^p) \quad (2)$$

2.1 Damage initiation phase

According to the benchmark [5], in the compression half-plane, the *activation function* is the straight line forming the Coulomb friction angle μ with the horizontal axis and passing through the point $(0, c_0)$ where c_0 is the peak cohesion.

In the traction half-plane the benchmark recommends a negligible tensile strength. For numerical reasons, this value was assumed $\chi_0 = c_0/10$. The shape of the activation function is parabolic with tangent continuity across the vertical axis (see [5]).

The convex domain inside the activation function constitutes the region of elastic behaviour of the joint, characterized by a 2×2 diagonal matrix K_{n0}, K_{t0} .

The point where damage initiation occurs is called fictitious crack tip (shortened FCT). During the evolutionary process, it moves from the upstream edge to the downstream edge.

2.2 Damage evolution phase

Once the activation function is achieved, irreversible displacements \dot{w}^p can develop along the interface. The effective inelastic displacement w^{eff} proposed by [3] is used:

$$\dot{w}^{eff} = \|\dot{w}^i\| = \sqrt{\dot{w}_n^2 + \dot{w}_t^2} \quad (3)$$

as kinematic internal variable driving the softening.

The inelastic displacement \dot{w}^i is the sum of plastic (unrecoverable) and fracture (recoverable in tension only) displacements \dot{w}^p and \dot{w}^f respectively. Total displacement discontinuities w are obtained by adding the elastic term to the previous ones:

$$w = w^e + w^p + w^f \quad (4)$$

Since w^f enters explicitly in the expression of damage parameter D , while w^p does not, a distinction between the two inelastic terms is necessary.

The traction-displacement discontinuity relationship reads as follows:

$$\dot{p} = \rho K_0 \dot{w}^e = \rho K_0 (\dot{w} - \dot{w}^p) \quad (5)$$

The matrix of elastic stiffness coefficients K_0 is pre-multiplied by coefficient ρ that is always equal to one in compression, and ranges from one to zero in tension according to the level of damage D as follows:

$$\rho = 1 - \frac{|p_n| + p_n}{2|p_n|} D \quad (6)$$

Damage D is defined as the complement to one of the ratio between the current normal stiffness K_{nc} and the initial one K_{n0} .

$$D = 1 - \frac{K_{nc}}{K_{n0}} \quad (7)$$

In order to compute K_{nc} a virtual configuration or equivalent uniaxial case is considered in which only normal inelastic displacements have occurred:

$$w_n^i = w^{eff} \quad (8)$$

It is furthermore assumed that a constant portion γ of the inelastic displacement w_n^i is represented by the unrecoverable plastic displacement w_n^p :

$$w_n^p = \gamma w_n^i \quad (9)$$

With the hypotheses formulated above, it is possible to compute K_{nc} (equation 4) and to take into account the fact that in mode I (without unloading) the value of the normal traction p_n coincides with the current normal strength χ function of the softening variable w^{eff} .

$$K_{nc} = \frac{p_n}{w_n - w_n^p} = \frac{\chi(w^{eff})}{w_n^e + w_n^p + w_n^f - w_n^p} = \frac{\chi(w^{eff})}{\frac{\chi(w^{eff})}{K_{n0}} + (1 - \gamma) w^{eff}} \quad (10)$$

Finally:

$$D = 1 - \frac{\chi(w^{eff})}{\chi(w^{eff}) + (1 - \gamma) w^{eff} K_{n0}} \quad (11)$$

The way in which tensile strength and cohesion deteriorate with increasing effective inelastic displacement is specified by means of monilinear softening curves:

$$\chi(w^{eff}) = \chi_0 \left(1 - \frac{w^{eff}}{w_{\chi_0}} \right) \quad (12)$$

$$c(w^{eff}) = c_0 \left(1 - \frac{w^{eff}}{w_{c_0}} \right) \quad (13)$$

where χ_0 represents the initial tensile strength (for $w^{eff} = 0$), c_0 the initial cohesion (for $w^{eff} = 0$), \mathcal{G}_F^I mode I fracture energy, \mathcal{G}_F^{IIa} asymptotic mode II fracture energy, w_{χ_0} value of w^{eff} for which tensile strength reaches zero (1.035 mm) and w_{c_0} the value of w^{eff} for which cohesion reaches zero (1.035 mm).

3 WATER PRESSURE IN THE PROCESS ZONE

In the process zone the water pressure is assumed as proportional to the damage level D . It means that the pressure at the real crack tip is the same as the pressure acting in the reservoir at the same depth. This pressure vanishes at the fictitious crack tip.

4 EXAMPLE OF APPLICATION

As an example of application, the benchmark problem proposed in 1999 by the International Commission On Large Dams [5] was analysed (dam height 80m, base 60m). The gravity dam and the rock foundation were discretized through 4693 and 7295 plane strain 3-node triangles, respectively. In the area where the fracture process zone is expected the element side is approximately 0.06 m. Tables 1 and 2 show the material properties assumed.

5 NUMERICAL RESULTS

The dam is analysed under self-weight, reservoir filling and imminent failure flood loading conditions. Since the joint is the weakest part in the structure, the remaining material behaves in a linear elastic way. Figures 1, 2, 3 and 4 are normalized by using c_0, w_{c_0} .

Material parameter	Rock	Concr.
Density [kg/m ³]	2700	2400
Tensile strength [MPa]	2.6	1.3
Softening law	linear	linear
Young modulus [MPa]	41000	24000
Poisson's ratio [-]	0.10	0.15
Mode I fracture energy [N/m]	200	150

Table 1: Material properties.

Material parameter	Mean values
Normal stiffness [MPa/mm]	45
Shear stiffness [MPa/mm]	20
Peak cohesion [MPa]	0.7
Residual cohesion [MPa]	0.0
Tensile strength [MPa]	0.07
Friction angle [deg]	30
Dilatancy angle [deg]	10

Table 2: Rock concrete interface properties.

5.1 *Self-weight loading*

In self-weight loading conditions, the dam and the foundation are perfectly tied together along the zero-thickness joint. The stresses induced along the joint for this mutual constraint are everywhere in elastic range. Therefore no displacement discontinuity occurs.

5.2 *Reservoir filling*

For simplicity, during this phase the hypothesis of proportional loading was assumed. Therefore, at the beginning of this phase, when the reservoir is empty, the external load multiplier vanishes. At the end of this phase, when the water level achieves the dam crest, the external load multiplier achieves the value of 1.

Figures 1 and 2 show displacement and stress histories at a point located at 0.12 m from the upper edge of the joint in the case of efficient impervious membrane (dry fracture) and in the case of water penetrating the crack (pressurized fracture), respectively. In order to reduce the size of both figures, the compressive stresses, which are negative, are plotted as positive. In the former case the decompression occurs for an external load multiplier of 0.67. In the latter case this value reduces to 0.63. Both values are very small due to the conservative assumption that the joint tensile strength is negligible ($\chi_0 = c_0/10$). In both cases the activation function is achieved in a tensile half-space so that tangential peak stresses are smaller than χ_0 .

In the case of pressurized fracture (Fig. 2), when the water level achieves the dam crest (external load multiplier of 1) the crack is stress free. For the same load level the dry crack is not yet stress free. In order to obtain a fully developed process zone, the water level overtopping the dam load

case is analysed.

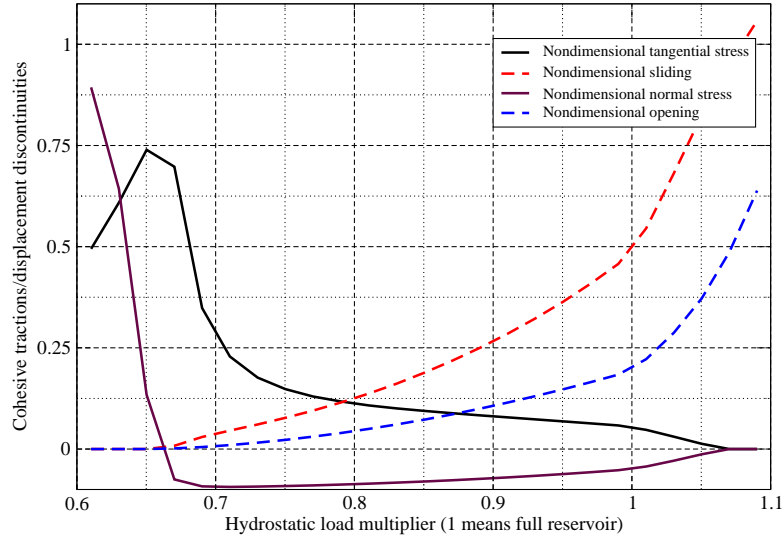


Figure 1: Tip response at 0.12 m from upstream side vs. load multiplier (dry fracture).

5.3 Imminent failure flood

This load case induces a uniform increment in the water pressure acting on the upper edge of the dam. In order to preserve the tangent continuity of the external load multiplier through the value of 1, it was assumed that a value of 1.1 corresponds to an overtopping water height of 0.1 the total dam height ($0.1 \times 80 = 8$ m).

Figures 3 and 4 show displacement and stress histories at a point located at 2 m from the upper edge of the joint in the case of efficient impervious membrane (dry fracture) and in the case of water penetrating the crack (pressurized fracture), respectively. In order to reduce the size of both figures, the compressive stresses, which are negative, are plotted as positive. In the former case the activation function is achieved in tensile half-space so that tangential peak stresses are smaller than χ_0 . In the latter case the activation function is achieved in the compressive half-space so that tangential peak stresses are larger than χ_0 , due to Coulombian friction. In both cases the condition of stress free crack is achieved during this load case.

6 COMPARISON WITH COULOMBIAN FRICTIONAL CRACK

Recently Karihaloo and Xiao [6] proposed to enrich the set of functions included in a finite element mesh by using an analytical solution based on the assumption that the two components of the cohesive stress are proportional. This enrichment can be applied in the framework of the so-

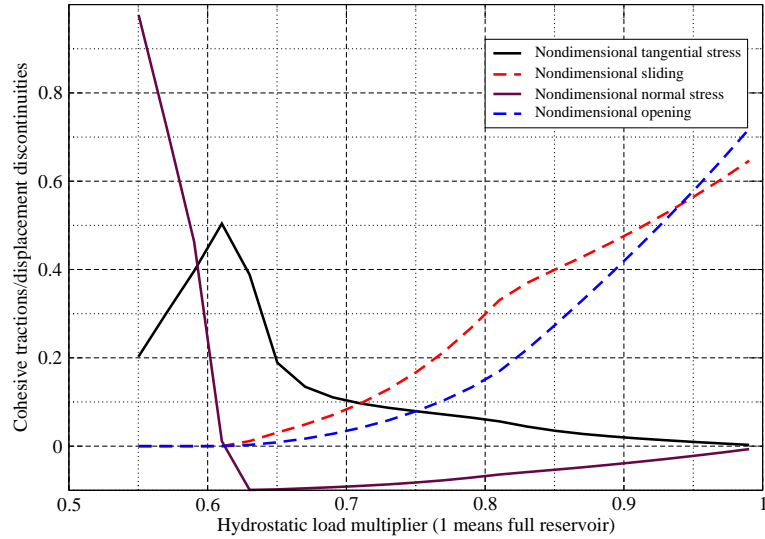


Figure 2: Tip response at 0.12 m from upstream side vs. load multiplier (pressurized fracture).

called XFEM/GFEM method. Figures 1, 2, 3 and 4 show at the fictitious crack tip a strong gradient in tangential stress and a small gradient in normal stress. Of course, this gradient is related to the time domain but, for the quasi-self-similarity of the problem, the same stress gradient appears in the space domain. At the real crack tip the hypothesis of cohesive proportional stress appears more realistic. Since the smallest eigenvalue of the tangential stiffness matrix is very small, it appears that, for the same load level, more than one solution is possible. Therefore, we will not be surprised if some small change in the mechanical model makes it possible to extend this proportionality condition from the real crack tip to the fictitious one.

7 CONCLUSIONS

- The reference volume involved in the fracture process of a dam joint is so large that it cannot be tested in a laboratory. Therefore this interaction has to be simulated numerically.
- Independently of the hydro-mechanical coupling, as the fictitious process zone moves from the upstream to the downstream edge, a transition occurs in the path of crack formation: the initial phase is dominated by the opening displacement, afterwards the shear displacement dominates.
- A judicious choice of the mechanical parameters required by the CKS joint model allows us to determine a stress and displacement field at the crack tip that is admissible according to the ICOLD benchmark from both a static and a kinematic point of view.

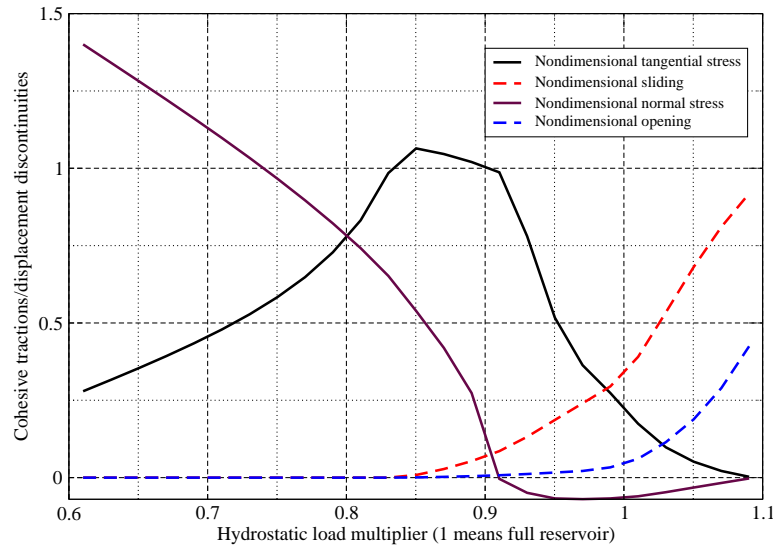


Figure 3: Tip response at 2 m from upstream side vs. load multiplier (dry fracture).

- For the same set of mechanical and geometrical data, the hydro-mechanical coupled fracture problem is more brittle than the dry one. The effect of the pressurized water is not only an obvious reduction in the load carrying capacity but also a reduction in the length of the process zone.
- During a laboratory test, the process zone at peak load is not completely developed. On the contrary, in real problems, at peak load not only the process zone is completely developed, but also a crack propagation under quasi-constant load occurs. In this case the ratio between the largest and the smallest eigenvalue of the tangent stiffness matrix tends to infinity and causes a slow rate of convergence in the Newton-Raphson process.

8 ACKNOWLEDGMENTS

The financial support provided by the Italian Department of Education, University and Scientific Research (MIUR) to the research project on “*Structural monitoring, diagnostic inverse analyses and safety assessments of existing concrete dams*” (grant number 20077ESJAP_003) is gratefully acknowledged.

References

- [1] A. Gens, I. Carol, and E.E. Alonso. A constitutive model for rock joints, formulation and numerical implementation. *Computers and Geotechnics*, 9:3–20, 1990.

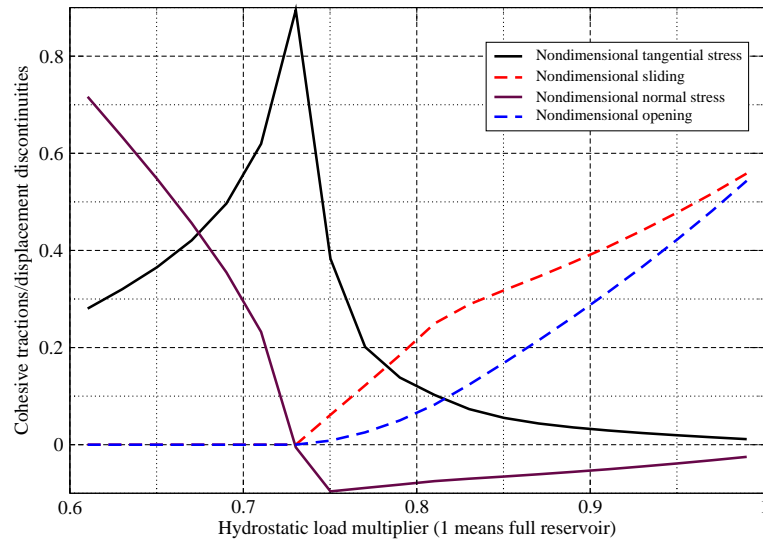


Figure 4: Tip response at 2 m from upstream side vs. load multiplier (pressurized fracture).

- [2] I. Carol, P.C. Prat, and C.M. Lopez. A normal/shear cracking model: Application to discrete crack analysis. *Journal of Engineering Mechanics (ASCE)*, 123(8):765–773, 1997.
- [3] J. Červenka, J.M.C. Kishen, and V.E. Saouma. Mixed mode fracture of cementitious bimaterial interfaces; part II: Numerical simulations. *Engineering Fracture Mechanics*, 60(1):95–107, 1998.
- [4] F. Barpi and S. Valente. Modeling water penetration at dam-foundation joint. *Engineering Fracture Mechanics*, 75/3-4:629–642, 2008. Elsevier Science Ltd. (Great Britain).
- [5] ICOLD. Theme A2: Imminent failure flood for a concrete gravity dam. In *Fifth International Benchmark Workshop on Numerical Analysis of Dams*, Denver (CO), 1999.
- [6] B.L. Karihaloo and Q.Z. Xiao. Asymptotic fields at the tip of a cohesive crack. *International Journal of Fracture*, 150:55–74, 2008.